IJE TRANSACTIONS C: Aspects Vol. 28, No. 9, (September 2015) 1359-1367

International Journal of Engineering

Journal Homepage: www.ije.ir

Optimal Design of Magnetorheological Fluid Damper Based on Response Surface Method

M. H. Djavareshkian*, A. Esmaeili, H. Safarzadeh

Department of Mechanical Engineering, Ferdowsi University of Mashhad, Mashhad, Iran

PAPER INFO

Paper history:
Received 12 August 2014
Received in revised form 14 June 2015
Accepted 03 September 2015

Keywords:
Magnetorheological Fluid
Damper
Optimization
Neuro-fuzzy
Particle Swarm Optimization
Response Surface Method

ABSTRACT

In this research, the effect of shape parameters such as number of magnet wire turns, spools, thickness of the gap, and pole length in a Magnetorheological (MR) fluid damper is analytically investigated and the optimization of these parameters is done with response surface method (RSM) which is combined Neuro-Fuzzy method and Particle Swarm Optimization (PSO) algorithm. Since the electromagnetic and mechanical components of a Magnetorheological (MR) fluid damper have a direct effect on the electrical power consumption, time delay, and damped force that are considered as objective functions. Because of the nonlinear behavior of the components, a robust approach is needed to predict their reactions; therefore, Neuro-Fuzzy is utilized to generate a high accurate surface and PSO finds the optimum solution base on the surface. The sensitive analysis is also performed to examine the variation of the objective functions with various input parameters. In this process, the best parameters are obtained by overtaking the appropriate value of the objective functions. The results demonstrate that the optimum MR damper has provided the best configurations, so that damps a maximum force in minimum time and lowest power consumption. On the other hand, the amplitude of vibrations is significantly decreased in the presence of the optimized MR damper.

doi: *10.5829/idosi.ije.2015.28.09c.14*

1. INTRODUCTION

Today's Magnetorheological (MR) fluid damper is widely utilized in industries. In this damper, MR fluids are applied, and viscosity of the fluid dramatically changes in the presence of an electric or magnetic field, leading to their being referred to as smart fluids. Due to the high ability of the MR fluids, they play a significant role in the area of damping systems. Consequently, many studies have been performed on this new damper. For instance, the results of groundbreaking research on the control of structural vibration [1], automotive suspension systems [2], and include the areas of aerospace industries [3], and seismic protection of bridge truss buildings [4] broadly support the view. After many investigations about MR damper, it is found that an accurate design of MR damper can highly influence on its performance [5]. In this design, some factors are more important and fundament, the design of an MR damper which minimizes the electrical power consumption and time delay and increases damped force is highly recommended such as a vital goal. On the other hand, the MR damper parameters are different in various applications, and there always exist a trade-off. Hence, many studies are done by several methods to design an MR damper with the high performance. Gavin et al. [6] have applied a method that minimizes the electrical power consumption and the inductive time constant while meeting a variety of conditions regarding the device's force capacity, size, and electrical characteristics. Another way can be using a magnetic FEM program to evaluate the magnetic properties of the candidate valves [7]. So, Nguyen et al. [8] have studied an optimal design of MR valves via an optimization procedure using a golden section algorithm and a local quadratic fitting technique which is constructed via a finite element method considering control energy and a

*Corresponding Author's Email: *javareshkian@ferdowsi.um.ac.ir* (M. H. Djavareshkian)

Please cite this article as: HM. H. Djavareshkian, A. Esmaeili,H. Safarzadeh, Optimal Design of Magnetorheological Fluid Damper Based on Response Surface Method, International Journal of Engineering (IJE), IJE TRANSACTIONS C: Aspects Vol. 28, No. 9, (September 2015) 1359-1367

time constant. Subsequently, Nguyen and Choi [9] have utilized this method to optimize a vehicle MR damper considering the damping force and dynamic range. Furthermore, this method is applied to the optimal design of MR shock absorber [10]. Elhami et al. [11] have utilized the fuzzy control theory and genetic algorithm, which optimizes fuzzy rules, to reduce the amplitude of vibrations. Also, Segla et al. [12] have optimized the dynamic behavior of the semi-active system with MR damper using genetic algorithms. Subsequently, a systematic method for the optimal analysis and design of MR damper elements is utilized [13]. Feng et al. [14] have studied about structural optimization of MR damper and a multi-objective optimization method, based on Parallel-plate Model and genetic algorithms, is proposed to obtain the optimal structural parameters for the MR damper. Furthermore, Jiang and Christenson [15] and Park et al. [16] have performed several investigations about the optimal design of MR damper.

In the present work, RSM method base on Neuro-Fuzzy and PSO method is introduced because of being simple, fast, more efficient, and useful for complex and nonlinear problem. Initially, the effects of shape parameters such as the number of magnet wire turns, spools, the thickness of the gap, and pole length in a Magnetorheological (MR) fluid damper is analytically investigated. Then, a high accurate design surface is anticipated by Neuro-Fuzzy, and the best solution is found according to PSO searching on the surface. Furthermore, sensitivity analysis is done, whereas cannot be seen in the many recent investigations. The paper is organized as follows. In section 2, a mathematical model of MR damper is outlined, and the underlying assumptions and notations are explained. In part 3, RSM method and how it works are described, and all stages of the processare quickly depicted. In section 4, the results of the study will be given, and the effect of shape parameters is investigated on the objective functions. For verification, the present results are compared with the experimental one. In section 5, comparative study of the smart damper is performed for various input parameters. In the last section, conclusions and future scopes of the work are provided.

2. MATHEMATICAL MODEL OF MR DAMPER

The damper has an electromagnetic piston that passes on MR fluid. MR fluids include micro-sized and magnetizable particles in a carrier fluid [17]. Piston magnet wire wrapped around a magnetic core is made up of fluid in the cylinder to create a magnetic flux. When a magnetic field passes through an MR fluid, it develops a yield stress, which must be achieved before the material flow. The piston is wrapped in magnet wires, and magnetic flux is generated in it, cylinder, and MR fluid. Subjected to intense magnetic fields, the yield stress of the MR increases. Hence, the damping force is increased by a factor of 10 or more. Figure 1 illustrates the conceptual design of the MR damper. The spools of magnet wire, shown in the vertical hash marks, generate magnetic flux within the steel piston. Adjacent spools are wound in opposing directions, and the magnetic flux forms three magnetic circuits. The flux in the magnetic circuit, flows axially through the steel core of diameter, beneath the windings, radially through the piston poles of length (L_p), through a gap of thickness (t_g), in which the MR fluid flows, and axially through the cylinder wall of thickness. The MR damper, designed in this paper, involves four different physically dimensioned parameters, thickness of the gap (t_g), length of pole (L_p), number of turn (N) and number of spool (N_s).

In the absence of an applied magnetic field, the particles in the MR fluid disperse randomly in a carrier fluid. MR fluid flows freely through the working gap between the fixed outer cylinder and rotor. MR fluid exhibits Newtonian-like behavior, and when the magnetic field is applied, the behavior of the fluid is often represented as a Bingham fluid having the variable yield strength. The shear stress of MR fluids can be described as:

$$\tau(B_g,\dot{\gamma}) = \tau_y(B_g)sgn(\dot{\gamma}) + \eta\dot{\gamma} \quad (1)$$

where, $\tau, \dot{\gamma}, B_g$ are shear stress, shear rate and magnetic flux density in the flow gap, respectivity. η is also viscosity of MR fluid with no applied magnetic field. In this study, it is assumed that the yield stress (τ_y) is proportional to the magnetic flux density (B), $\tau_y = \alpha B$ where $\alpha \approx 80\frac{Kpa}{T}$is material constant. The pressure reduction across the piston (Δp), depends on viscous and the yielding stress of fluid [17].

$$\Delta p = 2.1\frac{\tau_y}{t_g} + \Delta p_N \quad (2)$$

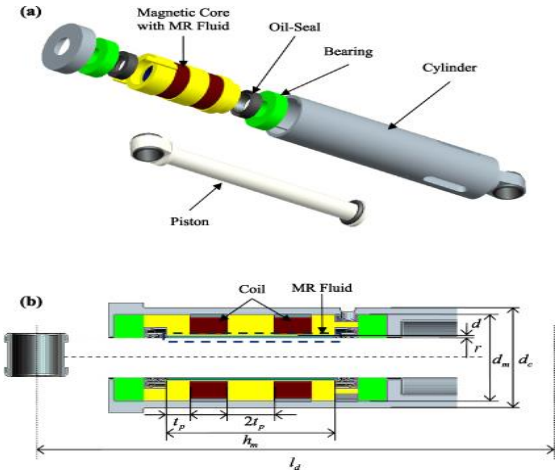

Figure 1. Diagram of the conceptual MR damper design

Δp_N is the viscous pressure loss and is approximated by:

$$\Delta p_N = \frac{12Q\eta(2N_s)L_p}{\pi(D_g+t_g)t_g^3} \quad (3)$$

where, Q, D_g are volumetric flow rate and diameter. The force generated in the device, F, is due to the pressure drop of fluid that it exists to pass the piston across the sectional area of the cylinder in every time, and it can be expressed as,

$$F = \Delta p\pi \times \frac{(D_p+t_g)^2-D_r^2}{4} \quad (4)$$

D_p, D_r are diameter of the piston and piston rod. For incompressible flow, Q is related to the piston velocity (V_p) by

$$Q = V_p(\pi/4)\left(D_p^2 - D_r^2\right) \quad (5)$$

Thus, the device force may be obtained from the piston velocity, the device geometry, the MR fluid properties and the magnetic flux density in the gap. The small volume of MR fluid between the cylinder wall and the piston's magnetic poles and between cylinder and piston are affected by the magnetic flux. The fluids that are between cylinder and piston have the maximum ratio of the magnetic field. This magnetic field can be analyzed using a magnetic Kirchhoff Law.

$$\sum_{j=1}^{k} H_j L_j = N_i \quad j = 1,2,\ldots,k \quad (6)$$

where, H_j is the magnetic field that is obtained from the number of links (k) and L_j is the effective length of the links. At the lower magnetic field, the flux density (B) is increased by magnetic inductance, $B = \mu\mu_0 H$, where μ_0 is the magnetic permeability of free space ($4\pi \times 10^{-7}$ T. m/A)[12] and μ is the relative permeability, which it depends on material properties. When the magnetic field becomes large, its ability to polarize the magnetic material is increased. At a threshold field, magnetic induction in the core (H_c), the material is almost magnetically saturated and the saturation magnetization (J_b) is obtained from:

$$J_b = B(H_c) + \mu H_c \quad (7)$$

In this study, the following relationship is utilized to describe the magnetization curves very well,

$$H(B) = \frac{H_c B}{J_b} + \frac{1}{2s} \times \left(\frac{1}{\mu_0} - \frac{H_c}{J_b}\right) \left(e^{arcsinh(s(B-J_b))} - e^{arcsinh(J_b)}\right) \quad (8)$$

where, s is sharpness of the B-H carve. The conservation of magnetic flux, $\emptyset_B$ is found from :

$$\emptyset_B = B_g A_g \quad (9)$$

$$B_c = \frac{\emptyset_B}{A_c} \quad (10)$$

$$B_w = \frac{\emptyset_B}{A_w} \quad (11)$$

B_g, B_c, B_w are magnetic flux density in the gap, core and wall, respectively and A_g, A_c, A_w are cross sectional areas of the gap, core and the cylinder wall, respectively. Now, the flux density for each component can be computed while the effect of magnetically saturated for every part is considered. By specifying B_g, the magnetic flux and flux densities in each component are calculated from Equations (8), (9), and (10). By giving magnetization parameters (B_c, J_b and s) for the steel and the MR fluid in the device, the magnetic induction is computed by Equation (7). By given B_g and H for each magnetic circuit component, the required current (I) can be obtained from the magnetic circuit equation:

$$I = \frac{1}{N}\left(2H_g t_g + H_c(l_c + l_P) + H_p\left(D_p + t_w\right) + H_w\left(l_c + l_p\right)\right) \quad (12)$$

where, H_g, H_w and H_p are magnetic induction in the gap, wall and the pole and l_c, l_P are also named as length of the core and pole; respectively. Moreover, t_w is the thickness of the cylinder wall. The inductance, L, resistance, R, voltage, V, and the inductive time constant, T_i, are determined by:

$$L = \frac{N_S N \emptyset_B}{I} \quad (13)$$

$$R = r \times N \times \pi \times D_c \times N_s \quad (14)$$

$$V = I \times R \quad (15)$$

$$T_i = \frac{L}{R} \quad (16)$$

where, r and D_c are resistance per unit length of the magnet wire and diameter of the core; respictively. The electrical energy consumption (J) is obtained from:

$$J = (\beta \times I \times R) \quad (17)$$

In the above equation, β is the weight coefficient. At high magnetic fields, magnetic materials become magnetically saturated very fast. To balance the electrical power and the flux density of the MR fluid, the magnetic field must be less than every part that becomes magnetically saturated. This design has some advantages such as the system operates in the low flux density. Therefore, it needs less magnetic field and fluid. Hence, the flux density in the steel is bounded by a maximum of 1.5 T (Tesla) [18]. The current cannot exceed the current rating of the wire.

1 The NIST reference on fundamental physical constants". Physics.nist.gov. Retrieved 2011-11-08

3. RESPONSE SURFACE METHOD (RSM)

In this study, RSM approach is introduced, so that is combined a Neuro-Fuzzy model [19-21] and Particle Swarm Optimization (PSO) [22, 23]. This method can be classified as a branch of surrogate methods, which applies Neuro-Fuzzy method to obtain design (or search) surface and PSO as an optimization algorithm. At first, the design variables, objective functions, and explicit inequality constraints are clearly explained in Table 1, and three objective functions and four design variables are considered, too. In the next step, initial sample selection is chosen by the design of experiment method, selection of points on the design surface at which the complete model is evaluated. Therefore, the analytical study is also done according to the initial selection, and the value of the objective functions are resulted and the obtained data are initially applied to training data.

Because of a nonlinear behavior between of the effective parameters (design variables) and objective functions and the unknown relationship between them, an intelligent system is required to identify this linkage. Moreover, the search surface should be determinate, and it is important to achieve a high precision of it. As a result, Neuro-Fuzzy method is utilized to find the most accurate search surface. Subsequently, the PSO algorithm tries to find the optimum solution in this design space and distributes its particles that constitute a swarm, moving around the search surface looking for the best solution and each individual flies in the search space with a velocity that is dynamically adjusted according to its own flying experience and its companions flying experience. This velocity is responsible for the movement imposed on the particle, changing its spatial location in the search of a better performance thereupon with these movements, the particles converge to the optimum position in search space and all of the particles almost move to a specified point so that it is found as an output of the algorithm. Next step is to evaluate the quality of design space based on the output of PSO and an additional analytical study. If the objective functions difference between the additional analytical investigation and the output satisfies the criteria, the process will be stopped; otherwise, the new analytical result is added to previous ones and then all steps will be performed again until the difference reaches a given threshold.

4. ANALYTICAL RESULTS AND VALIDATION

In this paper, the effects of shape parameters such as number of magnet wire turns, spools, thickness of the gap and pole length in a Magnetorheological (MR) fluid damper is analytically investigated and the optimization of these parameters is done by RSM approach, explained in the previous section. For analytical modeling, some conditions should be considered; for instance, magnetic materials become saturated very fast at high magnetic fields magnetically. To balance the electrical power and the flux density of the MR fluid, the magnetic field must be less than every part that magnetically becomes saturated. Therefore, it needs less liquid and magnetic field. Hence, the flux density in the steel is bounded by a maximum of 1.5 T. The current cannot exceed the current rating of the wire. Therefore, the wire gauge so that the following conditions are satisfied: $B_c<1.5$ T, $B_w<1.5$ T, F=(1KN~4KN), $(L_c+2L_p)\times N_s<0.25$m, $D_c<D_p-2T_c$, $I<I_{max}$ and V< 24volt. In these inequality constraints, T_c is the thickness of the coil winding, and I_{max} is the current rating of the wire. Therefore, the initial selection of design variables is done by the design of experiment method, Latin Hypercube Sampling (LHS) method [24]. According to the analytical model, a number of results are represented in Table 2(a)-(c) for the various number of turns of magnet wire (N), spools of wire (N_s), thickness of the gap (t_g) and piston poles of length (L_p).

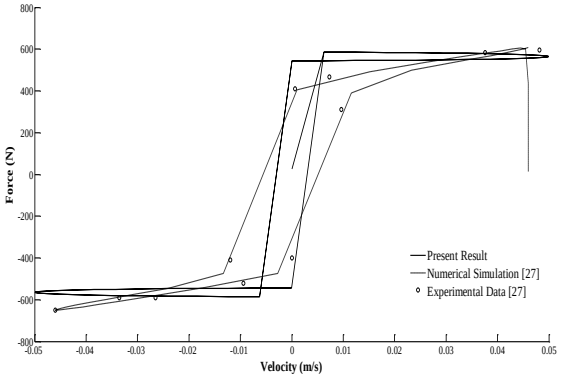

Figure 2. Comparison of damping force, according to the velocity between present analytical results, numerical simulation and experimental data [25].

TABLE 1. Description of design variables, objective functions, and constraints

Objective Functions	Design variables	Constraints
Time delay or time-consuming (T_c)	Number of turns of magnet wire (N)	$400 \leq N \leq 800$
Damped force (F)	Number of spools of wire (N_s)	$1 \leq Ns \leq 3$
Electrical power consumption (J)	Thickness of the gap (t_g)	$0.1 \leq t_g \leq 0.9$ mm
	Piston poles of length (L_p)	$1 \leq L_p \leq 4$ mm

TABLE 2. Results of analytical modeling for different N, N_s, t_g, and L_p.

	t_g=0.1			t_g=0.9		
N_s	F (N)	T_c (S)	J (j)	F (N)	T_c (S)	J (j)
1	6.75E+04	0.1117	5.1383	8.79E+02	0.0494	5.0759
2	1.34E+05	0.4673	10.5204	1.74E+03	0.2065	10.2596
3	2.00E+05	1.0972	16.1768	2.60E+03	0.4848	15.5644

(a) N=400, L_p=1

	t_g=0.1			t_g=0.9		
N_s	F (N)	T_c (S)	J (j)	F (N)	T_c (S)	J (j)
1	1.50E+05	1.95	7.73	1.37E+03	0.0842	7.624
2	2.99E+05	0.8381	15.9178	2.73E+03	0.3703	15.45
3	4.47E+05	2.0572	24.6766	4.09E+03	0.909	23.5285

(b) N=600, L_p=2.5

	tg=0.1			t_g=0.9		
N_s	F (N)	T_c (S)	J (j)	F (N)	T_c (S)	J (j)
1	2.33E+05	0.2844	10.3375	1.87E+03	0.1257	10.1788
2	4.64E+05	1.3003	21.4065	3.72E+03	0.5746	20.6808
3	6.95E+05	3.2915	33.4508	5.57E+03	1.4544	31.6137

(c) N=800, L_p=4

TABLE 3. Parameter for clustering genfis

Range of Influence	0.5
Squash Factor	1
Accept Ratio	0.5
Reject Ratio	0.15

The validity of the model and the system performance characteristics can be analyzed by computing the force, in terms of the various design variables explicitly. Initially, a part of these results is compared with numerical simulation and experimental data [24] which can be seen in Figure 2. The comparisons demonstrate that the present results are in a good agreement with published data, and the accuracy of the method is confirmed.

5. OPTIMIZATION RESULTS

In this step, design space approximation should be obtained. It is noteworthy that the analytical results demonstrate a nonlinear behavior between shape parameters (N, N_s, t_g, L_p) and objective functions (F, T_c, J). This problem is a multi-objective function, and every function has a weight coefficient so that they are assumed to be equal 1; then the sensitivity analysis updates the weights in next steps. Sensitivity is a measure of the contribution of an independent variable to the total variance of the dependent data. There are alternative approaches to sensitivity analysis, and Morris method is used in the present work. Its main purpose is to determine, within reasonable uncertainty, whether the effect of particular design variables is negligible, linear and additive or non-linear. In its simplest form, the empirical distribution of the sensitivities associated with each of the design variables (x_i) is estimated by computing a number ($2N_{dv}$) of first-order sensitivities of the model response with respect to each of the number of design variable (N_{dv}) at a set of random locations (p). More details can be found in [26].

Hence, the Neuro-Fuzzy model is applied to identify search space due to the non-linear manner. For the modeling, the number of turns of magnet wire (N), the number of spools of wire (N_s), thickness of the gap (t_g) and piston poles of length (L_p) are used as input and ($K=F/(J*T_c)$) ratio is utilized as output in Neuro-Fuzzy approach. A hybrid learning algorithm is employed for the model training, and the number of epochs is elected as 100. For the generation, sub clustering is applied, and the parameters for clustering genfis are in Table 3. The number of the membership function is 39 for each input, and the total rules are 2313441, (39×39×39×39), respectively. The type of the membership function is "gaussmf" and it is a symmetrical function.

The total number of data acquired at the time of this study is added up to 7533; all the above data have been collected by performing 7533 different analytical studies. For introducing the database to the model, it needs to be randomly broken down into two groups: training and testing. This new approach is trained by using the training set data; then the search surface is generated based on this information, and the test set is utilized to evaluate the predictive ability of the search surface generation. The training is continued as long as the computed error between the actual and predicted outputs for the test set is decreased. Typically, 75% of

the data is applied for training, and the rest are categorized as testing. The test set is used to evaluate the accuracy of the newly generated design space by providing the mentioned model for a set of data, which have been never considered, before. During the testing, the learning is turned off, and the chosen data set is fed into the model. The model output is collected, and a report is then generated for confirming the testing results. The efficiency of this approach is evaluated whenever the objective function values, obtained by analytical investigation, and the estimated ones, predicted by Neuro-Fuzzy, are compared. In addition, MSE, NMSE (Normalized Mean Squared Error), MAE (Mean Absolute Error) and R^2 (coefficient of determination) are applied as the other parameters for the calculation of error in this modeling. In brief, the accuracy of the generated search surface is verified if R^2, MAE, NMSE and MSE would be found to be close to 1, 0, 0 and 0, respectively. Table 4 illustrates the method performance in the terms of MSE, NMSE, MAE and the coefficient of determination R^2. The small value of the sundry error types, especially NMSE and high amount of R^2, particularly in the test, reveal the accuracy of the model. In Figures 3a and 3b, the predicted values of K versus the analytical ones are plotted for the training and testing data sets. The coefficient of determination is equal to 0.997 for training, whereas it is equal to 0.998 for the testing set, which are both well close to 1. The superior agreement between analytical data and search surface generation process indicates that it can be used as a powerful method for the surface generation. Therefore, a robust fuzzy knowledge based rules have been developed to predict damper performance. Finally, it was compared with the analytical data. Both analytical and predicted results are found to be valid within the acceptable limits.

TABLE 4. Neuro-Fuzzy performance values for train and test.

	MSE	NMSE	MAE	R^2
Train	0.000138	0.0023	0.007	0.997
Test	0.0001383	0.0024	0.0071	0.998

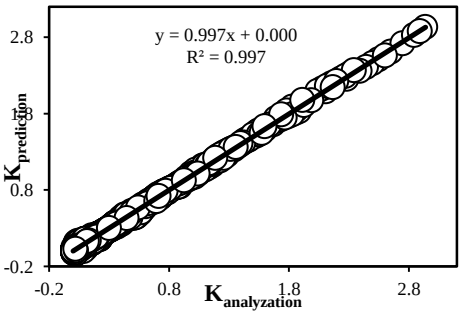

(a)

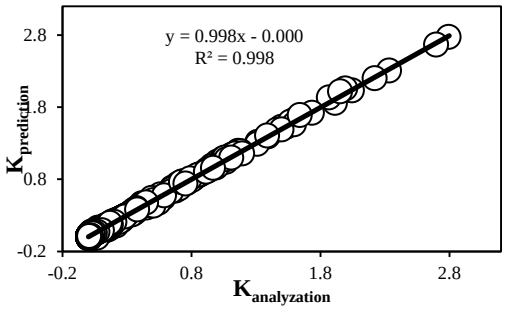

(b)

Figure 3. Results of analytical model versus predicted values of K: (a) Training data, (b) Testing data.

In the next step, the optimum solution has to be found by an optimization algorithm based on the search surface. An approximation of the optimal values (η_{app}) is obtained using PSO method, which determines the global maximizer of the constructed surfaces. For the design variables (i.e., N, N_s, t_g and L_p) resulted from the optimal solution, an additional analytical study is conducted to get η_{ana}, which is compared to η_{app}. The convergence criterion in Equation (18) decides if a new search surface is needed or not:

$$\varepsilon = \left|\frac{\eta_{ana}-\eta_{app}}{\eta_{app}}\right| \leq 10\% \quad (18)$$

In the case of a new surface is required, the interest region is systematically decreased and additional experiments are considered around to the latest point, found in the evaluation of η_{app}. In this study, only seven other search surfaces have been constructed until convergence is reached. Figures 4 and 5 demonstrate the 3D plots of the design space attained at the last optimization level with a final interest region range. In these figures, K is plotted versus turn (N), spool (N_s), gap (t_g) and L_P and it is apparently found the nonlinear behavior of the design variables and objective functions and the method captured all of them very well.

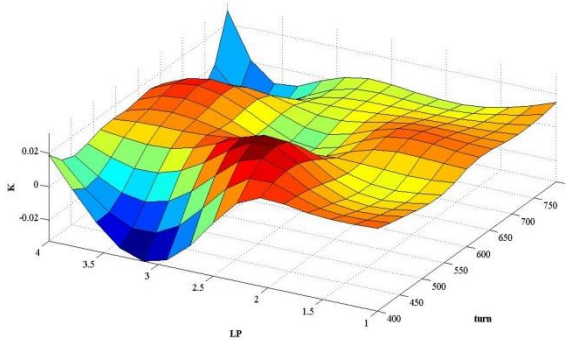

Figure 4. Generalization of the best-fitted search surface predicted by RSM based in turn, LP and K.

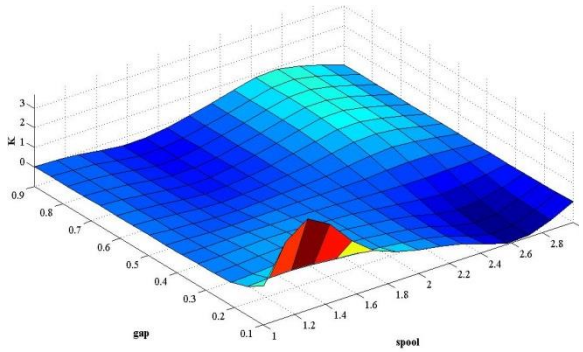

Figure 5. Generalization of the best-fitted search surface predicted by RSM based on the spool, gap, and K.

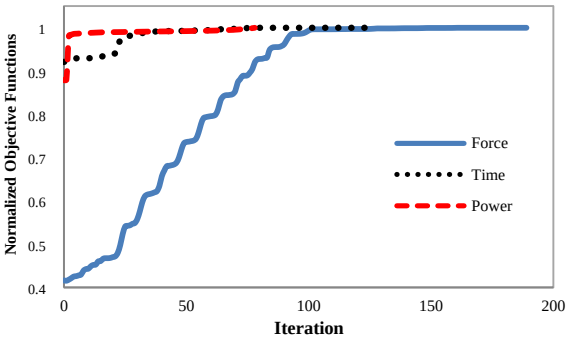

Figure 6. Evolution of three objective functions during the optimization process

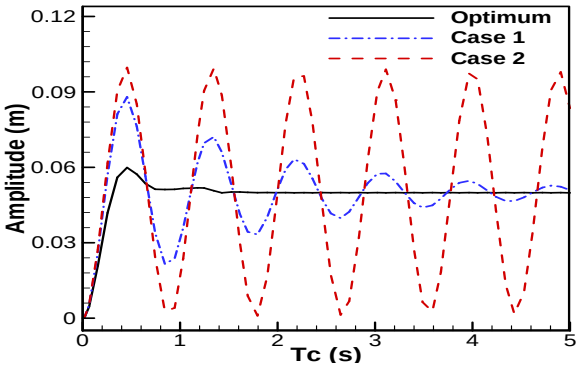

Figure 7. Variation of damper vibration as varying consuming time for optimized damper, case 1 and case 2.

TABLE 5. Characterization of the optimized damper

N	N_s	t_g	L_p	K
746	2	0.705	1.044	4.597

TABLE 6. The Best Value for Objective Functions

F (N)	T_c(s)	J (j)
4.7357×10^3	0.4483	19.1973

TABLE 7. Type of different MR damper and their characteristic.

Type of MR Damper	N	N_s	t_g	L_p
Optimum	746	2	0.75	1.044
Case 1	600	1	0.1	1
Case 2	800	3	0.9	4

Pursuant to following sentences, the best shape characteristics of MR damper are obtained by RSM method, and the optimal results are presented in Table 5. According to the present outcome, the best number of turns in a spool and the number of spools of wire should be equal to 746 and 2, respectively. Moreover, the optimum thickness of the gap should be also closed to 0.75 and the best piston poles of length are attained just over 1.044. The mentioned algorithm has estimated K=4.597 for this shape in the specified conditions. To validate the results of the algorithm, the analytical study at turn=746, spool=2, gap=0.705 and LP=1.044 has been performed, and the K coefficient value has been equal to 4.86. Therefore, the final error that is obtained by Equation (36) has been equal to 5.7%. According to the best value of MR damper, the damper force can be assessed in different electric flows. This damper has the best condition like the better damped force, minimum consumption electrical energy and fit size. The value of maximum electrical power, damped force, and delayed time of the optimum damper are illustrated in Table 6. To confirm the optimization process, the evolution of three objective functions is clearly depicted in Figure 6. The normalized value of them shows that all functions have been converged after some iteration. The significant point is that electrical power is quickly converged in a small iteration number when it is compared with the time and force. To verify the optimal design of MR damper, a comparison test between the optimized MR damper and two typical MR dampers is done. Table 7 demonstrates the characteristics of two conventional MR dampers.

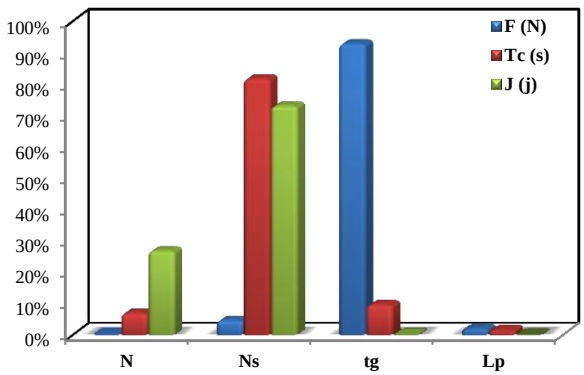

Figure 8. Sensitivity Analysis of the design variables in the objective functions

Furthermore, Figure 7 illustrates the amplitude of vibration according to the time consuming in optimized MR damper and traditional ones. Consequently, the figure shows that the best damper has the best performance and reduces the vibration.

6. SENSITIVITY ANALYSIS

In order to determine the performance of the smart damper working with Magnetorheological (MR) fluid, the sensitivity analysis of the effective parameters (N, N_s, t_g, L_p) is investigated on the objective functions (F, T, J). Subsequently, the percentage of their sensitivity is depicted in Figure 8. As it can be seen, the thickness of the gap (t_g) has impressed on force sharply, when it is compared with other design variables; moreover, the number of spools (N_s) has dramatically influenced on the time consuming (T) and electrical power (J), too. On the other hand, the number of turns (N) is more effectual on the electrical power (J), and the length of the pole (L_p) is generally the lowest effect. Consequently, it can be said that some parameters are most impressing in the design of MR damper.

7. CONCLUDING REMARKS

The effects of shape parameters such as the number of magnet wire turns, spools, thickness of the gap, and pole length in a Magnetorheological (MR) fluid damper are analytically investigated. The optimization of these parameters is also done with a new approach which combined Neuro-Fuzzy method and Particle Swarm Optimization (PSO) algorithm. Moreover, sensitivity analysis is performed, and the importance level of each design variable on the objective functions is regularly obtained. The main points of the research are:

1. The number of spools (Ns) have dramatically influenced on the time consuming (T_c) and electrical power (J), too.
2. The number of turns (N) is more effectual on the electrical power (J).
3. The length of the pole (Lp) is the lowest effect.
4. In summary, the optimum MR damper has provided the best conditions, so that damps a maximum force in a minimum time and most moderate power consumption. Moreover, the size of the new damper is so fitted and it reduces the vibration.

8. REFERENCES

1. Occhiuzzi, A., Spizzuoco, M. and Serino, G., "Experimental analysis of magnetorheological dampers for structural control", ***Smart Materials and Structures***, Vol. 12, No. 5, (2003), 703-711.
2. Shen, Y., Golnaraghi, M. and Heppler, G., "Semi-active vibration control schemes for suspension systems using magnetorheological dampers", ***Journal of Vibration and Control***, Vol. 12, No. 1, (2006), 3-24.
3. Lee, H.-S. and Choi, S.-B., "Control and response characteristics of a magneto-rheological fluid damper for passenger vehicles", ***Journal of Intelligent Material Systems and Structures***, Vol. 11, No. 1, (2000), 80-87.
4. Lee, T. and Kawashima, K., "Semi-active control of seismic-excited nonlinear isolated bridges", in Proc. 8th US National Conference on Earthquake Engineering, San Francisco, California, USA., (2006), 423, 421-429.
5. Xu, Z.D., Sha, L.F., Zhang, X.C. and Ye, H.H., "Design, performance test and analysis on magnetorheological damper for earthquake mitigation", ***Structural Control and Health Monitoring***, Vol. 20, No. 6, (2013), 956-970.
6. Gavin, H., Hoagg, J. and Dobossy, M., "Optimal design of mr dampers", in Proceedings of the US-Japan Workshop on Smart Structures for Improved Seismic Performance in Urban Regions. Vol. 14, (2001), 225-236.
7. Rosenfeld, N.C. and Wereley, N.M., "Volume-constrained optimization of magnetorheological and electrorheological valves and dampers", ***Smart Materials and Structures***, Vol. 13, No. 6, (2004), 13-23.
8. Nguyen, Q.-H., Choi, S.-B. and Wereley, N.M., "Optimal design of magnetorheological valves via a finite element method considering control energy and a time constant", ***Smart Materials and Structures***, Vol. 17, No. 2, (2008), 25-34.
9. Nguyen, Q.-H. and Choi, S.-B., "Optimal design of a vehicle magnetorheological damper considering the damping force and dynamic range", ***Smart Materials and Structures***, Vol. 18, No. 1, (2009), 15-28.
10. Nguyen, Q.-H. and Choi, S.-B., "Optimal design of mr shock absorber and application to vehicle suspension", ***Smart Materials and Structures***, Vol. 18, No. 3, (2009), 35-47.
11. Elhami, M.R., Daneshdoost, C. and Madady, D., Semi-active control of structure vibrations with mr damper using fuzzy control system (flc) and optimization through genetic algorithm (ga), in Advances in computer, communication, control and automation,(2012), Springer, 583-590.
12. Segla, S., Kajaste, J. and Keski-Honkola, P., Optimization of semi-active seat suspension with magnetorheological damper, in Vibration problems icovp (2011), Springer, 393-398.
13. Zhu, X., Jing, X. and Cheng, L., "Systematic design of a magneto-rheological fluid embedded pneumatic vibration isolator subject to practical constraints", ***Smart Materials and Structures***, Vol. 21, No. 3, (2012), 35-41.
14. Feng, Z., Hou, Z. and Zhang, G., "Multiobjective optimization of structural parameters designing for magnetorheological damper based on genetic algorithms", in 2011 International Conference in Electrics, Communication and Automatic Control Proceedings, Springer, (2012), 1455-1460.
15. Jiang, Z. and Christenson, R., "A fully dynamic magneto-rheological fluid damper model", ***Smart Materials and Structures***, Vol. 21, No. 6, (2012), 65-72.
16. Parlak, Z., Engin, T. and Çallı, İ., "Optimal design of mr damper via finite element analyses of fluid dynamic and magnetic field", ***Mechatronics***, Vol. 22, No. 6, (2012), 890-903.
17. Dominguez, A., Sedaghati, R. and Stiharu, I., "Modeling and application of mr dampers in semi-adaptive structures", ***Computers & Structures***, Vol. 86, No. 3, (2008), 407-415.
18. Steinmetz, C.P., "Theory and calculation of electric circuits, McGraw-Hill, Vol. 5, (1917).

19. Djavareshkian, M. and Esmaeili, A., "Neuro-fuzzy based approach for estimation of hydrofoil performance", ***Ocean Engineering***, Vol. 59, (2013), 1-8.
20. Park, S. and Rahmdel, S., "A new fuzzy sliding mode controller with auto-adjustable saturation boundary layers implemented on vehicle suspension", ***International Journal of Engineering-transactions C: Asp***, Vol. 26, No. 12, (2013), 1401-1410.
21. Bahramifara, A., Shirkhanib, R. and Mohammadic, M., "An anfis-based approach for predicting the manning roughness coefficient in alluvial channels at the bank-full stage", ***International Journal of Engineering-Transactions B: Application,*** Vol. 26, No. 2, (2013), 177-186.
22. Kennedy, J., Particle swarm optimization, in Encyclopedia of machine learning,(2010), Springer, 760-766.
23. Hashemi, F. and Mohammadi, M., "Combination continuous action reinforcement learning automata & pso for design of pid controller for avr system", ***International Journal of Engineering-Transactions A: Basics***, Vol. 28, No. 1, (2014), 52-63
24. Nahvi, H. and Mohagheghian, I., "A particle swarm optimization algorithm for mixed variable nonlinear problems", ***International Journal of Engineering***, Vol. 24, No. 1, (2011).
25. Liao, W. and Lai, C., "Harmonic analysis of a magnetorheological damper for vibration control", ***Smart Materials and Structures***, Vol. 11, No. 2, (2002), 288-296.
26. McKay, M.D., Beckman, R.J. and Conover, W.J., "A comparison of three methods for selecting values of input variables in the analysis of output from a computer code", ***Technometrics***, Vol. 42, No. 1, (2000), 55-61.

Optimal Design of Magnetorheological Fluid Damper Based on Response Surface Method

M. H. Djavareshkian, A. Esmaeili ,H. Safarzadeh

Department of Mechanical Engineering, Ferdowsi University of Mashhad, Mashhad, Iran

P A P E R I N F O

Paper history:
Received 12August 2014
Received in revised form 14 June 2015
Accepted 03 September 2015

Keywords:
Magnetorheological Fluid
Damper
Optimization
Neuro-fuzzy
Particle Swarm Optimization
Response Surface Method

چکیده

در این تحقیق، اثر پارامترهای شکلی همانند تعداد سیم پیچ های مغناطیسی، تعداد اسپول، ضخامت فاصله و طول پیستون در دمپر مگنتورولوژی به صورت تحلیلی مطالعه و بررسی می شود و بهینه سازی این پارامترها به روش پاسخ سطح انجام می شود به طوری که این روش ترکیبی از مدل Neuro-Fuzzy و الگوریتم بهینه سازی ازدحام ذرات است. از آنجایی که اجزاء الکترومغناطیسی و مکانیکی یک دمپر الکتروروولوژیکی اثر مستقیمی بر انرژی الکتریکی مصرفی، زمان دمپ و نیروی دمپ شده دارند لذا آن ها به عنوان تابع هدف در نظر گرفته شده اند.به خاطر رفتار غیر خطی این پارامترها، یک روش بسیار قوی مورد نیاز است تا رفتارهای آن ها را پیش بینی کند؛ به همین دلیل، روش Neuro-Fuzzy برای تولید یک سطح بسیار دقیق استفاده می شود و الگوریتم بهینه سازی ازدحام ذرات نیز حل بهینه را بر اساس این سطح جستجو می کند. همچنین آنالیز حساسیت برای دست یابی به میزان حساسیت تغییرات توابع هدف با تغییر پارامترهای ورودی انجام می شود. در این فرایند، بهینه ترین پارامترها به وسیله دستیابی به مقادیر مناسب توابع هدف بدست می آیند. نتایج نشان می دهد که دمپر MR بهینه بدست آمده، بهترین پیکره بندی را دارد به طوری که ماکزیمم نیرو را در حداقل زمان ممکن و بامصرف کم ترین مقدار انرژی دمپ می کند. از طرف دیگر، دامنه نوسانات این دمپر بهینه شده به شکل بسیار مناسب کاهش می یابد.

***doi**: 10.5829/idosi.ije.2015.28.09c.14*